ADVANCED MATERIALS

[1] J. Y. Ying, C. P. Mehnert, M. S. Wong, *Angew. Chem. Int. Ed.* **1999**, *38*, 56.
[2] S. Polarz, M. Antonietti, *Chem. Commun.* **2002**, 2593.
[3] A. H. Lu, W. Schmidt, A. Taguchi, B. Spliethoff, B. Tesche, F. Schuth, *Angew. Chem. Int. Ed.* **2002**, *41*, 3489.
[4] M. Kang, S. H. Yi, H. I. Lee, J. E. Yie, J. M. Kim, *Chem. Commun.* **2002**, 1944.
[5] J. Y. Kim, S. B. Yoon, J. S. Yu, *Chem. Mater.* **2003**, *15*, 1932.
[6] M. Choi, R. Ryoo, *Nat. Mater.* **2003**, *2*, 473.
[7] Y. Idota, T. Kubota, A. Matsufuji, Y. Maekawa, T. Miyasaka, *Science* **1997**, *276*, 1395.
[8] I. A. Courtney, J. R. Dahn, *J. Electrochem. Soc.* **1997**, *144*, 2045.
[9] H. W. Yan, S. Sokolov, J. C. Lytle, A. Stein, F. Zhang, W. H. Smyrl, *J. Electrochem. Soc.* **2003**, *150*, A1102.
[10] J. M. Tarascon, M. Armand, *Nature* **2001**, *414*, 359.
[11] M. Behm, J. T. S. Irvine, *Electrochim. Acta* **2002**, *47*, 1727.
[12] N. C. Li, C. R. Martin, *J. Electrochem. Soc.* **2001**, *148*, A164.
[13] I. A. Courtney, J. R. Dahn, *J. Electrochem. Soc.* **1997**, *144*, 2943.
[14] Y. W. Xiao, J. Y. Lee, A. S. Yu, Z. L. Liu, *J. Electrochem. Soc.* **1999**, *146*, 3623.
[15] S. Jun, S. H. Joo, R. Ryoo, M. Kruk, M. Jaroniec, Z. Liu, T. Ohsuna, O. Terasaki, *J. Am. Chem. Soc.* **2000**, *122*, 10712.
[16] B. Z. Tian, X. Y. Liu, B. Tu, C. Z. Yu, J. Fan, L. M. Wang, S. H. Xie, G. D. Stucky, D. Y. Zhao, *Nat. Mater.* **2003**, *2*, 159.
[17] T. Wang, Z. N. Ma, F. Xu, Z. Y. Jiang, *Electrochem. Commun.* **2003**, *5*, 599.
[18] H. Li, X. J. Huang, L. Q. Chen, *Electrochem. Solid State Lett.* **1998**, *1*, 241.
[19] I. A. Courtney, W. R. McKinnon, J. R. Dahn, *J. Electrochem. Soc.* **1999**, *146*, 59.
[20] M. Egashira, H. Takatsuji, S. Okada, J. Yamaki, *J. Power Sources* **2002**, *107*, 56.
[21] A. Ulus, Y. Rosenberg, L. Burstein, E. Peled, *J. Electrochem. Soc.* **2002**, *149*, A635.
[22] L. H. Shi, H. Li, Z. X. Wang, X. J. Huang, L. Q. Chen, *J. Mater. Chem.* **2001**, *11*, 1502.

Size-Dependent Periodically Twinned ZnSe Nanowires**

By *Quan Li*,* *Xingao Gong*, *Chunrui Wang*, *Juan Wang*, *Kitman Ip*, and *Suikong Hark*

ZnSe (bulk crystal $E_g = 2.7$ eV at 300 K)[1] is one of the key materials for applications in short-wavelength optoelectronics devices such as blue laser diodes (LDs), light-emitting diodes (LEDs), and photodetectors.[2] ZnSe-based microstructures have been widely investigated in recent years for their potential optoelectronic applications in high-density optical storage, full-color displays, etc.[3] Moreover, ZnSe exhibits significantly larger exciton binding energy (21 meV[4]) in comparison with that of GaAs (4.2 meV[5]), which makes it an ideal candidate for efficient room-temperature exciton devices and devices with improved temperature characteristics.[1] Controlling the size and the dimension of ZnSe, as well as achieving a confined interface induced by structure modulations, may further lead to novel properties.[6] Inspired by this, several groups have fabricated various ZnSe-based nanostructures such as quantum dots and nanorods (nanowires).[7]

In this paper, we report the fabrication of size-dependent periodically twinned ZnSe nanowires via the vapor–liquid–solid (VLS) mechanism. Alternating twins with specific periodicities are observed along the nanowire axial direction throughout the whole length of the wire. The twinning periodicity is linearly proportional to the diameter of individual nanowires. The formation mechanism of these periodically twinned ZnSe nanowires is discussed. The sharp excitonic peaks observed in the photoluminescence study reveal the high purity and structural order of these nanowires in spite of the large surface associated with the nanowire configuration and interfaces induced by the twin modulations. The high quality of the electronic structure demonstrates their potential as building blocks for optoelectronic nanodevices.

The nanowires were grown using a high-temperature tube furnace, and the experimental details can be found in the Experimental section. Light yellowish wool-like products were obtained on the alumina substrate downstream of the tube furnace. The X-ray diffraction (XRD) pattern of the products is shown in Figure 1a. All the diffraction peaks can be indexed to ZnSe (both zinc-blende (cubic) and wurtzite (hexagonal) phase) within experimental error. Figure 1b shows a low-magnification transmission electron microscopy (TEM) image of the as-fabricated material, which demonstrates the wire-like morphology of the product. These nanowires have a moderate size distribution, with the diameter ranging from 30–150 nm. Dark particles are located at the tips of most nanowires (as marked by the arrows in Fig. 1b). Alternating light/dark contrast appears in a periodic manner along most (> 90 %) of the wires' axial direction. The selected area electron diffraction (SAED) pattern taken from a typical nanowire indicates the existence of twinning (shown in the inset of Fig. 1b). Energy dispersive X-ray (EDX) spectra (Fig. 1c) taken from the tip and the wire region indicate the composition to be an Au-Zn-Se alloy and ZnSe, respectively.

High-resolution TEM images (Fig. 2) of individual nanowires suggest that the periodic light/dark contrast (in the low-magnification image) results from alternating twins along the cubic ZnSe <111> crystalline direction, which is the growth direction of these nanowires. It is interesting to note that, for the more than one hundred nanowires examined, the nanowire diameter (D) varies as the twinning period (P) changes. Figures 2a–2l are typical low-magnification TEM images of

[*] Prof. Q. Li, Dr. C. Wang, J. Wang, K. Ip, Prof. S. Hark
Department of Physics, The Chinese University of Hong Kong
Shatin, New Territory; Hong Kong (P.R. China)
E-mail: liquan@phy.cuhk.edu.hk
Prof. X. Gong
Surface Physics Laboratory & Department of Physics
Fudan University
200433 Shanghai (P.R. China)

[**] The work was supported by the RGC direct allocation of the Chinese University of Hong Kong under project Nos. 2060249 and 2060238, and a RGC grant under project Nos. CUHK 4247/01P and 4009104.

  DOI: 10.1002/adma.200306648

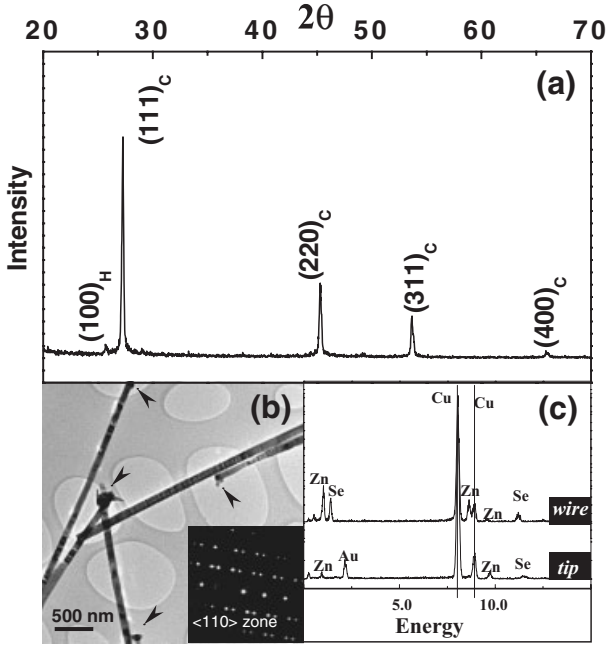

Figure 1. a) X-ray diffraction of the as-synthesized products revealing the existence of cubic and a small mount of hexagonal ZnSe. b) Low-magnification TEM image of several ZnSe nanowires with a dark particle at the tip and alternating light/dark contrast throughout the length of the wire. The selected area diffraction pattern (shown in the inset) taken from a typical nanowire suggests the existence of twinning in the nanowire. c) EDX spectra taken at the tip and wire region of the nanowires shown in (b).

such nanowires with diameter ranging from 150 nm (in Fig. 2a) to 36 nm (in Fig. 2l) with ±5 nm error. This error is mainly introduced due to the fact that the surfaces of these nanowires are not smooth at the atomic scale and a ~3 nm surface contamination layer (which is very common in nanowires grown by thermal evaporation) is usually present. The corresponding twinning period of these nanowires changes from 12.0 nm (in Fig. 2HR-a) to 1 nm (in Fig. 2HR-l), as clearly demonstrated by the high-resolution images. As the twinning periodicities of the individual nanowires are measured from the high-resolution TEM images, which give a much better measurement accuracy, the measurement error of P is estimated as ±0.1 nm. Nevertheless, fluctuation of the twinning periodicity within individual nanowires as well as within nanowires of similar diameters is detected. The largest fluctuation incurred in the current investigation is ≃1 nm, based on examination of P within individual nanowires and several other nanowires of approximately the same diameter. Therefore, the error of P is determined to be ±1 nm. The variation of P as a function of D is plotted in Figure 3, including error bars for both P and D. A linear relationship was identified between them, i.e., P is proportional to D. It is also observed that well-defined periodical twins are usually found in nanowires with larger diameters (>60 nm), the occurrence of the twins becomes a bit irregular as the nanowire diameter further shrinks (as shown in Fig. 2HR-j to HR-l).

A small number of nanowires (~10 % in the as-synthesized products) demonstrate fairly uniform contrast in the low-magnification image (Fig. 4a). The high-resolution image (Fig. 4b) taken from this type of nanowire reveals its hexagonal crystalline structure and the growth direction as the hexagonal [0002] crystalline direction. As with the cubic ZnSe nanowire, an Au-Zn-Se alloy tip is also present at one end of the nanowire.

The ZnSe nanowires are grown via the VLS mechanism,[8] as suggested by the experimental observation that an Au-Zn-Se alloy tip is always present at one end of the nanowire. All of the nanowires grow along a universal direction, which is perpendicular to the closest packed planes of ZnSe, i.e., {111} planes in the case of cubic ZnSe and {0001} planes for hexagonal ZnSe. Such a growth direction usually results from VLS growth, as it is regulated by the low interfacial energy between the closest packed planes and the liquid alloy.[9] The nanowires have a relatively large size distribution (30–160 nm in diameter), which may also be explained by another characteristic of the VLS mechanism—the diameter of the nanowire is consistent with the Au alloy particle size at the tip.[10] Due to the relatively high deposition temperature (~1100 °C), hexagonal ZnSe nanowires are also formed, which may be ascribed to the small energy difference between the hexagonal and the cubic phase (5.3 meV/atom).[11] In fact, a similar phenomenon has been observed by Ma et al. during their research on ZnS nanostructures.[12]

The linear correspondence between the twinning period and the nanowire diameter may be explained using a simple model by assuming a cylindrical configuration of the nanowires with cross-sectional diameter D. The surface of the cylinder can be treated as curved from a flat plane. The elastic energy per unit length (E) of the cylinder can be written as $E = 4\pi C/D$, where C is constant describing the elastic properties and the surface energy of the specific material. Governed by the VLS mechanism, the ZnSe phase would continuously precipitate out from the liquid Au alloy, allowing storage of the elastic energy (E) in the small volume of the solid ZnSe phase. The occurrence of the twins can be treated as periodic insertion of stacking faults into the lattice.[13] The stored elastic energy can be released by producing a stacking fault, associated with a stacking fault energy γ, leading to the relation $E \times P \sim \gamma$, where P is the periodicity for the appearance of a stacking fault. This results in the linear dependence of the twinning periodicity on the nanowire diameter (Eq. 1):

$$P \sim \frac{\gamma}{4\pi C} D \tag{1}$$

Nevertheless, various kinetic growth factors could affect twin formation and introduce unavoidable fluctuations of the twinnning periodicity (Fig. 3) in individual nanowires and between nanowires with approximately the same diameter.[14]

The nanowire-specific growth direction <111> as determined by the VLS mechanism, together with the cubic structure, which allows {111} planes as stacking fault (twinning) planes, are prerequisite conditions for the formation of the

ADVANCED MATERIALS

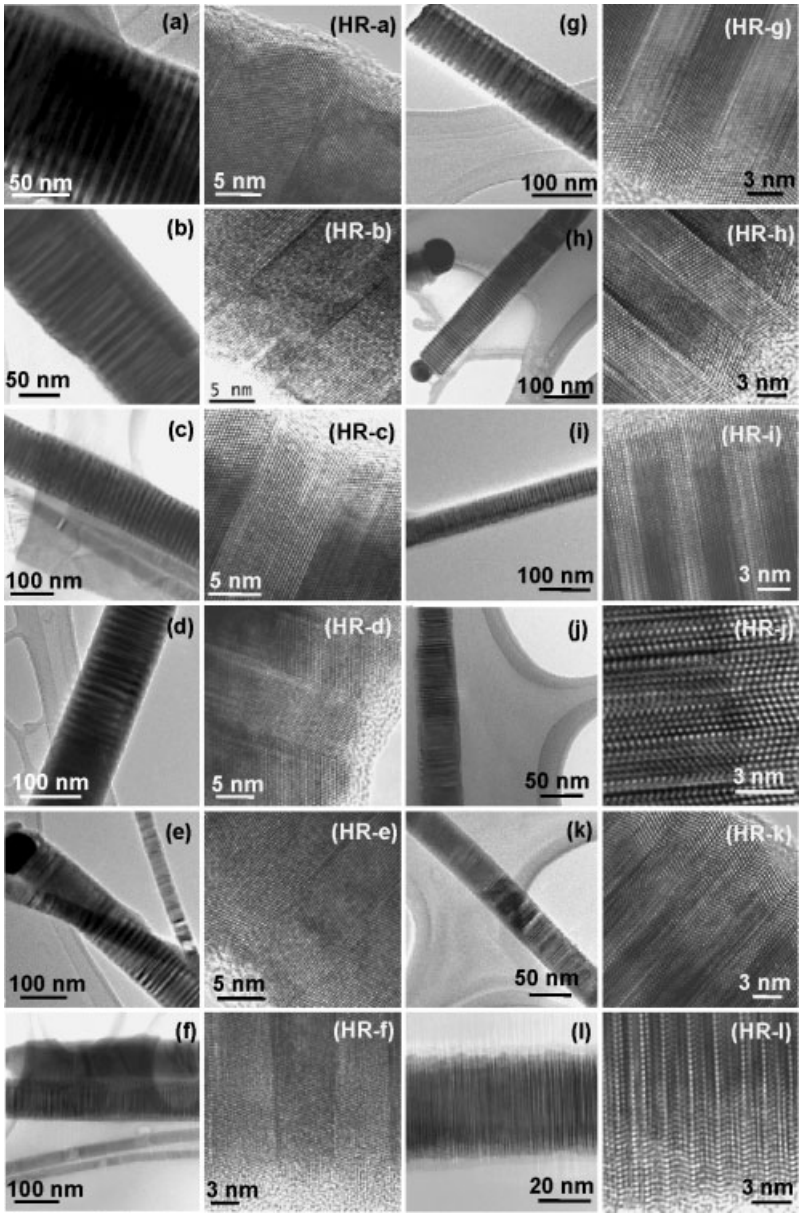

Figure 2. a–l) Low-magnification TEM images of ZnSe nanowires with periodical light/dark contrast, with diameter 150 nm, 132 nm, 120 nm, 112 nm, 100 nm, 90 nm, 80 nm, 72 nm, 58 nm, 52 nm, 45 nm, and 36 nm, respectively. HR-a–HR-l) The corresponding high-resolution images of the ZnSe nanowires shown in (a–l), revealing a decreasing twinning periodicity of 12 nm, 9.9 nm, 8.5 nm, 8.1 nm, 7.1 nm, 6.9 nm, 4.9 nm, 4.6 nm, 2.6 nm, 1.9 nm, 1.9 nm, and 1.0 nm, respectively.

periodical twinning configuration as described above. The requirement of a specific crystalline plane serving as the twinning plane, together with the VLS determined growth direction, eliminates the possibility of generating similar twins in the ZnSe nanowires with hexagonal structure, which is consistent with the experimental observations.

Figure 5 shows the room-temperature and low-temperature (10 K) photoluminescence (PL) spectra of the as-synthesized nanowires. While the room-temperature spectrum only gives a thermally broadened band edge emission at ~2.7 eV and a broad defect-related emission centered at ~2.0 eV, the low-temperature PL spectrum is dominated by the excitonic emissions, which are blue shifted and split into three characteristic peaks. The peak I_1^d at 2.778 eV can be readily attributed to bound excitons at a deep donor 42 meV[15] beneath the valence band, given that the bandgap of cubic ZnSe is 2.820 eV at 10 K.[16] The band-to-acceptor (BA) peak at 2.751 eV indicates an acceptor binding energy of 70 meV. The other peak at 2.722 eV can be ascribed to emission from donor–acceptor pair (DAP) transitions associated with a donor having a ~28 meV binding energy. The acceptor and donor possibly come from trace impurities in the source materials during the thermal evaporation process.[17] The two weak emissions centered at 2.384 eV and 1.998 eV involve Al impurity[18] and self-activated defects,[19] respectively. Due to the high growth temperature of the nanowires and usage of alumina as the substrate material, a trace amount of Al impurity may diffuse into the nanowire through surface diffusion and contribute to the deep level emissions. Although the excitonic peaks are slightly broadened and not well-resolved, which is possibly caused by the proximity of the complexes to the surface and the interfaces associated with the multiply twinned nanowire configuration,[20] the dominant excitonic feature in the spectrum unambiguously demonstrates the high quality of the electronic structure of these nanowires. The weak shoulder at the higher energy of 2.836 eV (see inset of Fig. 5) is assigned to the bound excitons of the hexagonal phase (with a bandgap of 2.874 eV), which is consistent with the observation of a small amount of hexagonal ZnSe in the same sample.

In conclusion, cubic (zinc-blende) ZnSe nanowires with periodically alternating twins along the wire growth direction have been synthesized using thermal evaporation in the presence of Au catalyst. These nanowires were grown via a VLS mechanism, and the relatively large size distribution (diameter 30 to 160 nm) is primarily ascribed to the size distribution of the Au droplet. In the current system, the periodicity of the alternating twins has a linear dependence on the diameter of the nanowires. Such a periodical occurrence of twinning is driven by the elastic energy stored in a cylindrical portion of the nanowire when it precipitates out from the liquid alloy droplet during nanowire growth. The specific crystalline structure (zinc-blende in this case) and the corresponding crystal growth direction (<111> direction here) are necessary conditions for multiple twin generation. Sharp excitonic peaks, which dominate the

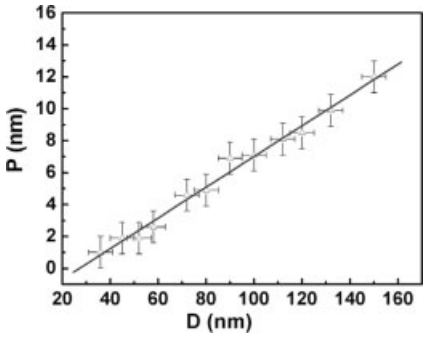

Figure 3. The twinning periodicity (*P*) as a function of the nanowire diameter (*D*), based on the experimental results shown in Figure 2. The error bar of *P* represents a 15 nm measurement error, and that of *D* represents a 1 nm fluctuation.

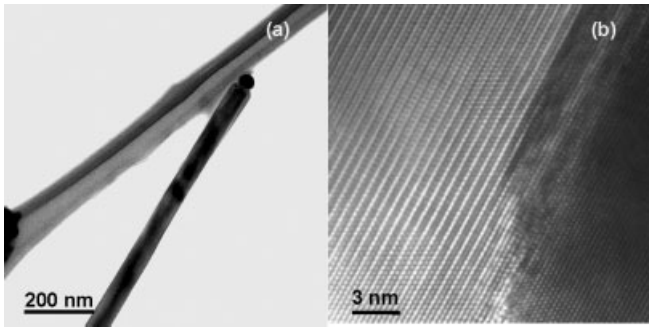

Figure 4. a) Low-magnification TEM image of a ZnSe nanowire without the periodical light/dark contrast along the growth direction. b) High-resolution image of the corresponding nanowire in (a), revealing its hexagonal structure.

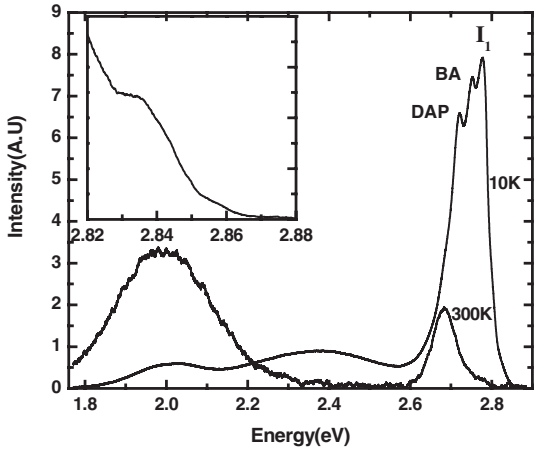

Figure 5. PL spectra of the ZnSe nanowires taken at room temperature and at 10 K. The inset shows the weak shoulder at 2.836 eV in the 10 K spectrum.

low-temperature PL spectrum of the nanowires, reveal the high quality of the electronic structure despite the large unpassivated surface and interface associated with the twinned nanowire configuration. As the twinning interface of the cubic ZnSe constitutes a complete unit cell of hexagonal ZnSe (with ABA stacking sequence, compared to ABCA stacking in the cubic phase), such periodically twinned nanowires constitute ideal quantum wells (alternating cubic and hexagonal phase with a difference in the bandgap, but not in chemical composition), which may have potential applications in nanoscience and technology.

Experimental

The nanostructures were grown using a high-temperature vacuum tube furnace, the setting of which is described elsewhere [8]. Briefly, the ZnSe powder was placed on an alumina boat in the central region of the alumina tube, and single-crystalline alumina (0001) substrates with a thin gold film on the surface were placed downstream of the tube. The tube was then pumped down to a base pressure of 2×10^{-2} torr. Pure Ar was introduced into the tube at a constant flow rate of 150 sccm. The total pressure was maintained at 300 torr during the fabrication process. The furnace was maintained at 1100 °C for 2 h before it was cooled down to room temperature.

The general morphology and crystallinity of the sample were examined by scanning electron microscopy (SEM, LEO 1450VP), and X-ray diffraction (XRD, Rigakau RU-300 with Cu $K\alpha_1$ radiation), respectively. The detailed microstructures of the sample were investigated using transmission electron microscopy (TEM). A Tecnai 20 microscope (FEG, operating at 200 kV) was employed for various TEM-related studies, and the energy dispersive X-ray (EDX) measurements were performed using an energy dispersive spectrometer (Oxford Instrument) attached to the same microscope. The PL spectra were measured from the sample mounted on a cold finger in a continuous cycle cryostat using the 325 nm line of a HeCd laser. The spectral resolution of the spectrometer was set at 250 μeV in all measurements. To more accurately extract the peak positions the obtained spectra were fitted with Gaussian peaks.

Received: December 18, 2003
Final version: March 12, 2004

[1] R. Rujkorakarn, A. J. Nelson, *J. Appl. Phys.* **2000**, *87*, 8557.
[2] a) T. Matasuoka, *Adv. Mater.* **1996**, *8*, 469. b) R. Pässler, E. Griebl, H. Ripel, G. Lautner, S. Bauer, H. Preis, W. Gebhardt, B. Buda, D. J. As, D. Schikora, K. Lischka, K. Papagelis, S. Ves, *J. Appl. Phys.* **1999**, *86*, 4403. c) J. Wang, D. C. Hutchings, A. Miller, E. W. Van Stryland, K. R. Welford, I. T. Muirhead, K. L. Lewis, *J. Appl. Phys.* **1993**, *73*, 4746.
[3] a) S. K. Hong, E. Kurts, J. H. Chang, T. Hanada, M. Oku, T. Yao, *Appl. Phys. Lett.* **2001**, *78*, 165. b) M. A. Haase, J. Qiu, J. M. Depuydt, H. Cheng, *Appl. Phys. Lett.* **1991**, *59*, 1272. c) H. Jeon, J. Ding, W. Patterson, A. V. Nurmikko, W. Xie, D. C. Grillo, M. Kobayashi, R. L. Gunshor, *Appl. Phys. Lett.* **1991**, *59*, 3619.
[4] Z. M. Zhu, N. Z. Liu, G. H. Li, H. X. Han, Z. P. Wang, S. Z. Wang, L. He, R. B. Ji, Y. Wu, *J. Infrared Millimeter Waves* **1999**, *18*, 13.
[5] S. Z. Wang, S. F. Yoon, L. He, X. C. Shen, *J. Appl. Phys.* **2001**, *90*, 2314.
[6] a) C. M. Lieber, *Nano Lett.* **2002**, *2*, 82. b) M. T. Bjork, B. J. Ohlsson, T. Sass, A. I. Persson, C. Thelander, M. H. Magnusson, K. Deppert, L. R. Wallenberg, L. Samuelson, *Nano Lett.* **2002**, *2*, 87. c) M. S. Gudiksen, L. J. Lauhon, J. F. Wang, D. C. Smith, C. M. Lieber, *Nature* **2002**, *415*, 617. d) Y. Wu, R. Fan, P. D. Yang, *Nano Lett.* **2002**, *2*, 83. e) Y. Jiang, X. M. Meng, J. Liu, Z. R. Hong, C. S. Lee, S. T. Lee, *Adv. Mater.* **2003**, *15*, 1195.
[7] a) S. W. Haggata, D. J. Cole-Hamilton, J. R. Fryer, *J. Mater. Chem.* **1997**, *7*, 1969. b) Y. F. Chan, X. F. Duan, S. K. Chan, I. K. Sou, X. X. Zhang, N. Wang, *Appl. Phys. Lett.* **2003**, *83*, 2665. c) T. Makino,

ADVANCED MATERIALS

R. Andre, J. M. Gerard, R. Romestain, L. S. Dang, M. Bartels, K. Lischka, D. Schikora, *Appl. Phys. Lett.* **2003**, *82*, 2227. d) B. Xiang, H. Z. Zhang, G. H. Li, F. H. Yang, F. H. Su, R. M. Wang, J. Xu, G. W. Lu, X. C. Sun, Q. Zhao, D. P. Yu, *Appl. Phys. Lett.* **2003**, *82*, 3330. e) Y. C. Zhu, Y. Bando, *Chem. Phys. Lett.* **2003**, *377*, 367. f) N. Kouklin, L. Menon, A. Z. Wong, D. W. Thompson, J. A. Woollam, P. F. Williams, S. Bandyopadhyay, *Appl. Phys. Lett.* **2001**, *79*, 4423.

[8] R. S. Wagner, in *Whisker Technology* (Ed: A. P. Levitt), Wiley-Interscience, New York **1970**, Ch. 3.

[9] A. M. Morales, C. M. Lieber, *Science* **1998**, *279*, 208.

[10] Y. Cui, L. J. Lauhon, M. S. Gudiksen, J. F. Wang, C. M. Lieber, *Appl. Phys. Lett.* **2001**, *78*, 2214.

[11] a) C. Y. Yeh, Z. W. Lu, S. Froyen, A. Zunger, *Phys. Rev. B* **1992**, *46*, 10 086. b) Z. L. Wang, M. Mohamed, S. Link, M. A. El-Sayed, *Surf. Sci.* **1999**, *440*, L809.

[12] C. Ma, D. Moore, J. Li, Z. L. Wang, *Adv. Mater.* **2003**, *15*, 228.

[13] R. Banerjee, R. Jayakrishnan, P. Ayyub, *J. Phys. Condens. Matter* **2000**, *12*, 10 647.

[14] Z. L. Wang, Z. R. Dai, Z. G. Bai, R. P. Gao, J. Gole, *Appl. Phys. Lett.* **2000**, *77*, 3349.

[15] K. Mochizuki, K. Masumoto, T. Yasuda, Y. Segawa, K. Kimoto, *J. Cryst. Growth* **1994**, *135*, 318.

[16] H. Venghaus, *Phys. Rev. B* **1979**, *19*, 3701.

[17] P. Yu, M. Cardona, in *Fundamentals of Semiconductors: Physics and Materials Properties*, Springer, Berlin **1996**, p. 159.

[18] S. Gezci, J. Woods, *J. Lumin.* **1975**, *10*, 267.

[19] S. Fujita, H. Mimoto, T. Noguchi, *J. Appl. Phys.* **1979**, *50*, 1079.

[20] F. T. Vasko, A. V. Kuznetsov, in *Electronic States and Optical Transitions in Semiconductor Heterostructures*, Springer, New York **1999**, p. 173.

Enzymatic Formation of Supramolecular Hydrogels**

By *Zhimou Yang*, *Hongwei Gu*, *Degang Fu*, *Ping Gao*, *Jing Kwok Lam*, and *Bing Xu**

Gels formed by three-dimensional elastic networks whose interstitial spaces are filled with liquid present many useful properties (e.g., response to external stimuli)[1] and applications in many areas (e.g., bioanalysis, chemical sensing, food processing, cosmetics, drug delivery, and tissue engineering).[2] Motivated by the existing and potential applications of gel materials, research on gels has expanded rapidly in the past two decades. In particular, non-polymeric gelators have been the focus of increasing research attention over the past two decades. Initially, small-molecule organogelators, which are low-molecular-mass molecules that self-assemble into fiber-like networks that encapsulate organic solvents to form organogels, received a lot of attention.[3] Subsequently, small molecules that form gels in water emerged.[4] The demonstration of self-assembled oligopeptides,[5–8] which gel in water and provide hydrogels for biomedical applications (e.g., as scaffolds to promote the growth of neurons,[8,9] to induce biomineralization,[5] or to assist cell adhesion[7]), has stimulated recent research efforts on low-molecular-weight hydrogelators.[10,11] Hydrogels formed from small molecules show many properties commonly observed in hydrogels made from natural or synthetic polymers, such as responses to pH change, thermal perturbation, and ligand-receptor interactions,[11] and their formation can be trigged by these stimuli. Recently, Hu and Messersmith reported the use of an enzyme to crosslink polymers to induce hydrogelation,[12] and Mooney and co-workers demonstrated the use of cells as crosslinkers for polymers to promote gelation.[13] Both methods are believed to be advantageous in the biomedical application of hydrogels. Similar methodologies, however, are yet to be explored with hydrogels formed by small molecules.

We report the use of an enzymatic reaction to convert an ionic group on an amino acid derivative into a neutral group, which creates a small-molecular hydrogelator and leads to the formation of supramolecular hydrogels. This gelation process utilizes an alkaline phosphatase—one of the components of kinase/phosphatase switches that regulate protein activity—to dephosphorylate the PO_4^{3-} of *N*-(fluorenylmethyloxycarbonyl) (FMOC) tyrosine phosphate (**1**) under basic conditions.[14] Unlike previously reported enzymatic gelation processes,[12] this process, which involves bond breaking rather than bond formation, adjusts the balance of the hydrophobicity and hydrophilicity of the precursor, a simple amphiphilic derivative of amino acids, to yield a hydrogelator. Since dephosphorylation is a common yet important biological reaction existing in many organisms, its coupling with hydrogelation may lead to a general and useful way to generate and utilize biomaterials based on supramolecular hydrogels.

Scheme 1 illustrates two typical procedures for inducing gelation by the dephosphorylation of **1**. In the first case, **1** and one equivalent of Na_2CO_3 are dissolved in a phosphate buffer (pH = 9.6) to form a clear solution (Fig. 1A). The addition of alkaline phosphatase converts the solution of **1** into an opaque hydrogel of **2** with a pH of 9.6 (Fig. 1B, gel **I**) at 37 °C in 30 min. In the second case, equal moles of **1** and **3** and two equivalents of Na_2CO_3 are mixed in the phosphate buffer (pH = 9.6) to form a suspension (Fig. 1C) upon gentle heating. The suspension is added to the alkaline phosphatase and kept at ~ 60 °C for 3 min. The suspension turns into a clear solution, which forms a clear hydrogel (Fig. 1D, gel **II**) upon cooling

[*] Prof. B. Xu, Z. Yang, H. Gu, Prof. D. Fu, J. K. Lam
Department of Chemistry
The Hong Kong University of Science & Technology
Clear Water Bay, Hong Kong (P.R. China)
Email: chbingxu@ust.hk
Prof. B. Xu
Bioengineering Program
The Hong Kong University of Science and Technology
Clear Water Bay, Hong Kong (P.R. China)
Prof. P. Gao
Department of Chemical Engineering
The Hong Kong University of Science and Technology
Clear Water Bay, Hong Kong (P.R. China)

[**] The authors acknowledge Hong Kong Research Grant Council, The Hong Kong University of Science Technology (EHIA), and E. I. DuPont Co. (Young Faculty Award to BX) for their financial support. We thank Ms. Pauline S. T Leung for help with rheology testing.

  DOI: 10.1002/adma.200400340